FUNCTION™ american physiological society

FUNCTION, 2022, 3(3): zqac020

https://doi.org/10.1093/function/zqac020
Advance Access Publication Date: 5 May 2022
Original Research

RESEARCH ARTICLE

Subcellular Propagation of Cardiomyocyte β-Adrenergic Activation of Calcium Uptake Involves Internal β-Receptors and AKAP7

Thomas R. Shannon[1,†], Dan J. Bare[1,†], Sabine Van Dijk[2], Shayan Raofi[2], Tiffany N.-M. Huynh[2], Yang K. Xiang[2,3], Julie Bossuyt[2], Kimberly L. Dodge-Kafka[4], Kenneth S. Ginsburg[2], Donald M. Bers[2,*]

[1]Department of Molecular Biophysics and Physiology, Rush University, Chicago, IL 60605, USA, [2]Department of Pharmacology, University of California-Davis, Davis, CA 95616, USA, [3]VA Northern California, Mather, CA 95655, USA and [4]Calhoun Center for Cardiology, University of Connecticut Health Center, Farmington, CT 06030, USA

*Address correspondence to D.M.B. (e-mail: dmbers@ucdavis.edu)
†These authors contributed equally to this study.

Abstract

β-adrenergic receptor (β-AR) signaling in cardiac myocytes is central to cardiac function, but spatiotemporal activation within myocytes is unresolved. In rabbit ventricular myocytes, β-AR agonists or high extracellular [Ca] were applied locally at one end, to measure β-AR signal propagation as Ca−transient (CaT) amplitude and sarcoplasmic reticulum (SR) Ca uptake. High local $[Ca]_o$, increased CaT amplitude under the pipette faster than did ISO, but was also more spatially restricted. Local isoproterenol (ISO) or norepinephrine (NE) increased CaT amplitude and SR Ca uptake, that spread along the myocyte to the unexposed end. Thus, local $[Ca]_i$ decline kinetics reflect spatio-temporal progression of β-AR end-effects in myocytes. To test whether intracellular β-ARs contribute to this response, we used β-AR-blockers that are membrane permeant (propranolol) or not (sotalol). Propranolol completely blocked NE-dependent CaT effects. However, blocking surface β-ARs only (sotalol) suppressed only ∼50% of the NE-induced increase in CaT peak and rate of $[Ca]_i$ decline, but these changes spread more gradually than NE alone. We also tested whether A-kinase anchoring protein 7γ (AKAP7γ; that interacts with phospholamban) is mobile, such that it might contribute to intracellular spatial propagation of β-AR signaling. We found AKAP7γ to be highly mobile using fluorescence recovery after photobleach of GFP tagged AKAP7γ, and that PKA activation accelerated AKAP7γ-GFP wash-out upon myocyte saponin-permeabilization, suggesting increased AKAP7γ mobility. We conclude that local β-AR activation can activate SR Ca uptake at remote myocyte sites, and that intracellular β-AR and AKAP7γ mobility may play a role in this spread of activation.

Submitted: 24 March 2022; **Accepted:** 28 April 2022

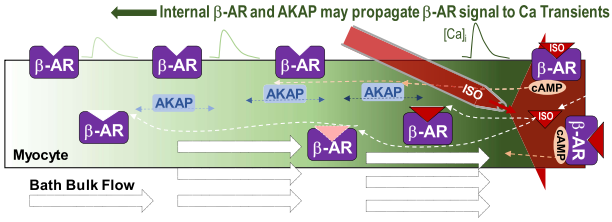

Key words: β-adrenergic signaling; sarcoplasmic reticulum; calcium transients; protein kinase A; A-kinase anchoring protein

Introduction

β adrenergic receptor (β-AR) stimulation of cardiac myocytes takes place through a well-defined series of steps starting with catecholamine binding to the receptor leading to G-protein activation.[1,2] and consequent adenylyl cyclase activity to generate cAMP which activates protein kinase A (PKA). Protein kinase A phosphorylates myocyte targets, including the L-type calcium (Ca) channel, phospholamban (PLN), which regulates the sarcoplasmic reticulum (SR) Ca-ATPase, and troponin I on the myofilaments and others to orchestrate increased contraction (inotropy) and lusitropy (relaxation).[2]

Myocyte β-AR responsiveness is diminished in disease states including heart failure (HF),[3,4] although basal sympathetic tone is increased in HF, which is usually treated with β-AR antagonists.[5] In addition, β-AR activation of PKA is typically highly localized via specific A-kinase anchoring proteins (AKAPs) to corresponding targets including L-type Ca channels (LTCC), PLN (on the SR), and myofilaments, with differential inhibition in hypertrophy and HF. A myocyte's global inotropic/lusitropic response to a particular β-AR agonist is shaped by multiple properties of the β-AR cascade, including which receptor subtypes are activated, the balance between cAMP diffusion and activation/breakdown by phosphodiesterases, localization, and abundance of phosphatase and specific AKAPs.[6–8] Thus, the β-AR response can be highly localized and the location of the machinery associated with the response correlates with changes in local function.[2,9]

But, as well-known as this series of events is, there is limited information on the spatio-temporal dynamics of the cascade within adult cardiomyocytes. Much has been learned using β-AR subtype-selective agonists, antagonists, and targeted sensors,[10–12] but paradoxes exist where imputed cAMP behavior and the role of AKAPs may be consistent with either relatively free diffusion or severe restriction within nanodomains. Nikolaev et al. showed that cAMP produced by strong local β_1-AR activation could diffuse through a myocyte but that cAMP produced by β_2-AR was more highly restricted.[13] In any case, how, exactly, the β-AR signal is transduced into end-effectors like the SR Ca-ATPase and myofilaments that are distributed throughout the cytosol has been little studied. Highly localized effectors inside the cell, as is typical for AKAP complexes, are critical in some cases such as LTCC.[7–9,14] This very local dedicated complex of proteins at AKAPs works well for ion channels, which are in low abundance and have high amplification factors (millions of ion per second), but would be costly for abundant cellular proteins like the SR Ca-ATPase and myofilaments (30–100 μM) that are widely dispersed and require relatively synchronous collective activation for their full functional effects. There is a knowledge gap as to how this is achieved.

The anchoring protein AKAP7 (specifically AKAP7γ or δ; also known as AKAP18γ or δ) is known to bind PLN and PKA,[7,15] but the mechanism by which this might expedite PLN phosphorylation is unknown. Recent data indicates that PLN phosphorylation decreases the PLN affinity of AKAP7γ, which also functions as a dimer.[15–17] The myocyte concentration of PLN (~100 μM) far exceeds that of PKA (0.1 μM),[16,18] such that dedicated anchoring of one PKA molecule near only 10 PLN molecules, would not suffice. This raises the a provocative hypothesis that AKAP7γ molecule mobility might increase with β-AR activation and translocate active PKA along the SR surface locally to facilitate rapid spatio-temporal SR Ca-ATPase activation.

It has also recently been shown that standing prelocalized intracellular α- and β-ARs bind catecholamines to generate local intracellular effects.[19–23] Norepinephrine (NE) uptake into mouse myocytes is mediated by organic cation transporter 3 (OCT3) and studies have revealed that in human HF NE reuptake is impaired.[24]

Whole-cell β-AR responses must be the superposition of responses initiated by receptors and cascade members at all locations within the myocyte. Conventional experiments with global agonist application neither mimic localized adrenergic neuron release nor inform how β-AR activity at individual microlocations[25] propagate over space and time to contribute to the whole response. Toward clarifying this, here we use a technique to activate β-AR locally at one myocyte location and measure the propagation of the local response away from that site via local $[Ca]_i$ dynamics. In addition, we test the involvement of internal β-AR receptors in the response using β-AR antagonists, which have differential membrane permeability. We also test AKAP7γ mobility within the myocyte and whether upon β-AR activation that mobility increases in such a way that it might assist in the spread of the β-AR response away from sites of activation. We conclude that internal signal propagation to increased SR Ca uptake occurs and that internalized receptors and mobile AKAP7γ may participate in spatial spread of the β-AR response.

Materials and Methods

Experiments were conducted in strict adherence to the guidelines for the care and use of experimental animals at Rush University Medical Center and at the University of California, Davis, and were approved by the Institutional Animal Care and Use Committees of each institution (Animal Welfare Assurance, A-3120-01). Rabbits were killed by exsanguination under verified deep anesthesia. Experiments were done within a few hours of cell isolation on a given day. All animals were euthanized under deep anesthesia via rapid thoracotomy and excision of the

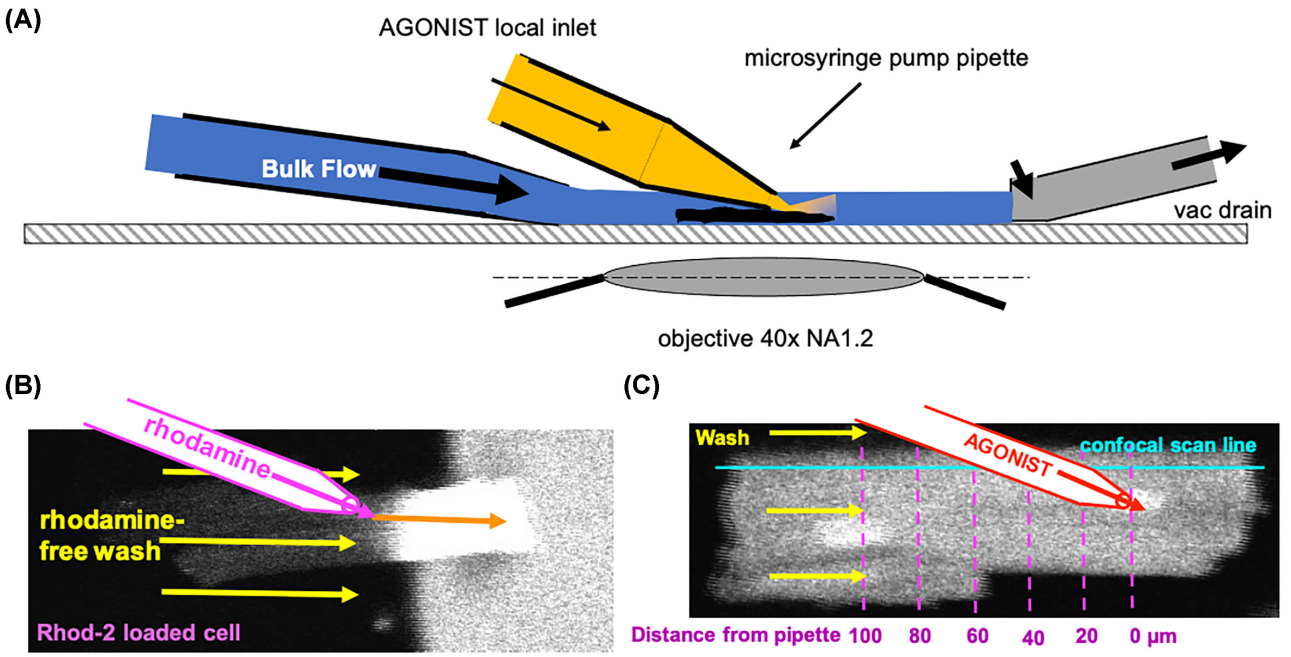

Figure 1. (A) Experimental set up. Myocyte was mounted on a coverslip on a confocal microscope stage. Control NT solution bulk flow (blue) is depicted from left to right from a pipette (diameter = 100 μm, 1 mL/min) located ≈2 mm upstream of (left of) the myocyte. A pipette loaded with agonist (diameter = 25–35 μm, 25 μL/min; gold) was placed immediately above (but not touching) the distal (downstream, right) end of the myocyte. Agonist is applied via a microsyringe pump. (B) To verify agonist flow, a rhod-2-AM loaded myocyte was exposed local application of rhodamine-B, observable as a bright end of the myocyte, but the background bulk flow washes the rhodamine away to the right preventing rhodamine access to the left end of the myocyte. (C) Experimental protocol for agonist application and Ca measurement in a rhod-2 loaded myocyte along the confocal scan line. Agonist pipette was centered transversely over a cell.

heart. Rabbits were anesthetized using pentobarbital (I.V. into the marginal ear vein). All efforts were made to minimize any potential suffering or pain experienced by the animals.

Ventricular myocytes were isolated from New Zealand white rabbit (Myrtle Rabbitry, Thompson Station, TN or Charles River, San Francisco, CA). Data were collected with PClamp (Axon Instruments, Foster City, CA). Mathematical data manipulation was performed using MATLAB (MathWorks Inc), Microsoft Excel (Microsoft Corporation), and GraphPad Prism (GraphPad Software, San Diego, CA). All experiments were conducted at room temperature (25°C).

Chemicals and reagents were purchased from Sigma Aldrich unless indicated. Normal Tyrode's (NT) solution was composed as follows (in mM): 2 Ca, 140 NaCl, 4 KCl, 1 $MgCl_2$, 10 glucose, 5 HEPES, and pH 7.4 with NaOH.

Calcium Measurements

Ventricular myocytes were isolated from New Zealand white rabbits using retrograde Langendorff perfusion with Liberase TM at 37°C as previously described.[26]

Our experimental set up for the described protocol was as depicted in Figure 1(A). Myocytes were plated on to a laminin-coated glass coverslip (No.1; 0.13–0.17 mm) with a rectangular well created with polymerized silicone for solution retention. The myocytes were then examined using a Zeiss LSM 510-META or Zeiss 5 Live inverted confocal microscope for high-speed laser scanning (Carl Zeiss Microscopy; White Plains, NY) with a 40 × water immersion objective.

Myocytes were loaded for 25–30 min with 10 μM of the Ca-dependent fluorescent indicator rhod-2-AM (Thermo Fisher Sci.; Waltham, MA). The cells were then washed and left to de-esterify for 20 min. Next, the coverslip/myocytes were transferred to the microscope stage and holder, perfused with NT solution containing (in mM) NaCl 140, KCl 4, $MgCl_2$ 1, and $CaCl_2$ 2 or as described later for specific experiments, and glucose 5.5, with pH buffered using HEPES 10 (as free acid and Na salt) to 7.4. Myocytes were external field stimulated at 0.5 Hz (≈25–50 V/cm × 2 ms). Fluorescence was measured at 590 nm in response to 543 nm excitation.

The coverslip with cells was continuously perfused with a "background" perfusion outlet placed at the rearmost location of the solution well and gravity feed from a NT reservoir, and vacuum aspiration from the front end. Another perfusion outlet (diameter 100 μm) with a well-controlled flow rate of 1 mL/min was also placed about 2–3 mm proximal to the cell. The two outlets allowed a "bulk" perfusion of NT over the entire cell (calculated linear velocity 2.12 m/s, affording laminar flow unlikely to move or dislodge cells) and prevented possible accumulation of test ligands during repeated trials. This solution was NT except where β-AR blockers (propranolol or sotalol) were included as indicated. Cells were paced for a minimum of 20 beats to achieve steady-state at the start of any experiment before agonist perfusion (below). Cells treated with 5 μM thapsigargin were preincubated before the beginning of the experiment for at least 25 min. Pretreatment with propranolol (1 μM) or sotalol (25 μM) was for at least 10 min.

An approximately 25–35 μm diameter glass micropipette with solution containing 2 μM isoproterenol (ISO) or 200 nM NE was placed at the distal end of the cell using a manually positioned micromanipulator, under visual control. ISO is lipophilic and membrane-permeant and can, thus rapidly enter cardiac myocytes, and will have access to both surface and any intracellular β-ARs. Norepinephrine is cationic and poorly membrane

permeant, but it is taken up via OCT (eg, OCT3), and therefore, can access both surface and intracellular β-ARs.[20,21] The perfusion pipette was attached to a solution filled gas-tight glass syringe with a stiff thick-walled PTFE line. Flow was regulated via a Legato-100 series syringe pump (KD Scientific Inc.; Holliston, MA), at a rate of 25 μL/min (calculated linear laminar flow velocity 0.35–0.7 m/s). The perfusion pipette was placed on the "downstream" end of the myocyte as the bulk Tyrode solution flow moved over the cell (from left to right in Figure 1A). The pipette tip was centered along the transverse axis of the cell, with the z-axis position approaching closely the top surface of the myocyte but not visibly contacting or indenting the membrane. Figure 1(B) shows agonist flow, visualized with 1 μM of fluorescing rhodamine-B placed in the perfusion pipette. Upon activation, rhodamine-B was continuously ejected over the distal end of the nondye loaded cell, and immediately washed forward and away by the bulk solution flow, thus leaving the entire portion of the cell upstream from the micropipette unexposed.

Experiments were generally performed as in Figure 1(C). Isolated rabbit myocytes were loaded with rhod-2-AM. A scan line (512 pixels) was placed longitudinally through the cell so that Ca-dependent fluorescence could be measured along the line. The pixel size was $<$ 0.2 μm, and taken into account during analysis of each experiment to render distances in μm. The scan duration was 2 ms/line (pixel dwell time 3.9 μs). The perfusion pipette loaded with agonist was placed as in Figure 1(B). and the distal portion of the cell was exposed. Local Ca or agonist perfusion was maintained at least as long as shown in the figures, 70 s or more. Measurements of the generated signal over time were made along the scan line, from immediately underneath the pipette and along the length of the cell, as the signal propagated up the cell into the unexposed areas. The confocal aperture was set to 3 Airy units and the focal plane was set in the interior of the cell, to provide a stable and not overly localized detection area and maintain signal to noise ratio, while at the same time preserving longitudinal axis resolution sufficient to detect agonist response dynamics. The resulting line scan was preliminarily smoothed over time with a 5-point Boxcar averaging algorithm (MATLAB). The resulting data were then background subtracted (based on fluorescence from a cell-free segment of the scan) and were averaged over a 25 μm distance, 12.5 μm on either side of each pixel (moving average). Background-subtracted and smoothed fluorescence data were converted to cytosolic free [Ca] ($[Ca]_i$) using a standard pseudoratio equation with single site binding and resting fluorescence assigned to $[Ca]_i = 100$ nM.

Recombinant DNA Constructs and Adenoviruses

We created recombinant DNA constructs and viral vectors with fluorescent labeled proteins for imaging experiments. To express fluorescently labeled proteins in rabbit cardiomyocytes, we created wild type AKAP7γ (AKAP-WT) tagged with GFP at the C'-terminus of the proteins. The Adeasy Adenoviral Vector System (Agilent Technologies) was used per the manufacturer's instructions to create an adenoviral vector with AKAP7γ-GFP. Adenoviral vector with PLN that was N'-terminally tagged with YFP was gifted by Dr. Robia from Loyola University.[27]

Fluorescence Recovery After Photobleach (FRAP)

Rabbit cardiomyocytes were plated on laminin-coated chambered cover glasses and cultured $<$ 28 h in M199 media to allow for adenoviral expression of either GFP tagged AKAP7γ or YFP-tagged PLN. At the onset of experiments, the culture media was replaced by NT solution (in mM: 140 NaCl, 1 $MgCl_2$, 5.5 glucose, 4KCl, 5 HEPES-Na, 5 HEPES-H free acid) with 2 mM Ca. Experiments were done at room temperature (22–23°C) on an inverted Nikon A1 confocal microscope (40x objective). Cardiomyocytes were excited at 488 nm with emission signal was recorded at 525 nm. For FRAP recordings, a circular region with a 10 μm diameter was bleached to reduce the fluorescent signal to 25%–35% of initial value. Fluorescence recovery was followed by recording images for up to 5 min when a plateau was reached.

Images were analyzed using ImageJ and the fluorescent intensity was then fitted with a two-phase association in Graphpad Prism.

Permeabilizing Cardiomyocytes

Cultured cardiomyocytes were permeabilized using saponin. Prior to this, cells were incubated $\geq$ 30 min with 80 μM cytochalasin D to inhibit myocyte contraction upon permeabilization. Myocytes were imaged on an inverted Nikon A1 confocal microscope (40x objective) to record fluorescence during and after myocyte permeabilization. Cells were rapidly permeabilized by 3 min exposure to 500 μg/mL saponin in internal solution which contained (in mM: 0.5 EGTA, 10 HEPES, 120 K-aspartate, 5 ATP, 5 phosphocreatine di-Na, 5 U/mL creatine phosphokinase, 10 reduced glutathione, and 8% dextran (Mr: 40 000). pH set to 7.2 with NaOH.). The saponin solution was then replaced with internal solution containing free $[Ca]_i = 100$ nM (calculated using MaxChelator) and loss of fluorescence was recorded for up to 50 min after the start of permeabilization. The loss of fluorescence was also measured after incubating cells with 10 μM Forskolin for 5 min prior to saponin exposure.

Results

Effects of Spatially Localized Increased Extracellular [Ca] Upon the Cardiac Myocyte

Figure 2(A) shows an example of the abrupt application of ISO on the downstream end of a rabbit ventricular myocyte, with the average global Ca transients shown at right. In order to first test the spatiotemporal effects of increasing Ca transients in a spatially restricted area of the cardiac myocyte without the involvement of β-AR, we locally applied elevated extracellular [Ca] (4 mM) through the agonist pipette at the downstream end of the myocyte (Figure 2B, inset). This allowed the higher $[Ca]_o$ to be washed away with NT, without exposing the myocyte upstream to the pipette $[Ca]_o$. Cells were paced at 0.5 Hz at least 20 times to bring them to steady-state before local $[Ca]_o$ elevation which was continued for typically 1–2 min.

Each trace in Figure 2(B) is the Ca transient at a given distance upstream of the pipette along the longitudinal scan line. In these control traces (left; 2 mM Ca, same as background flow), Ca transient peak amplitude declined slightly with increasing distance away from the pipette. During 4 mM Ca application (right), peak $[Ca]_i$ increased substantially, with the greatest increase directly under the pipette and progressively lesser increases as distance from pipette increased. The traces in each panel of Figure 2(B) are time-aligned well within 2 ms (duration of scan line from which x = 0–45 μm was extracted). The increase in Ca transient magnitude is highest just underneath the pipette (x = 0), averaging 60.7 ± 14.7% higher than the pre-Ca level at the same location (Figure 3A; $n = 7$). The increase in peak $[Ca]_i$ gradually declined

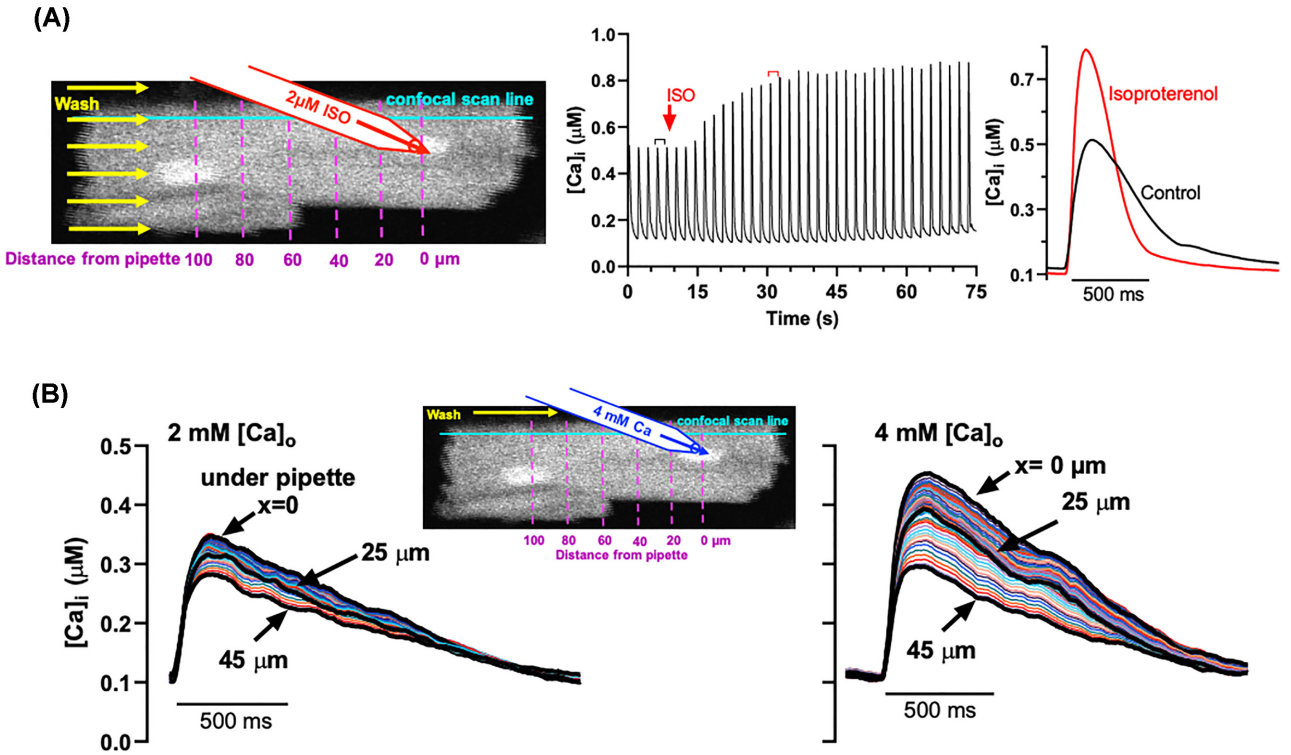

Figure 2. (A) Experimental protocol. The pipette was loaded with 2 μM ISO. A representative time course of Ca transients is shown at right. Upon local ISO application, peak $[Ca]_i$ grew progressively higher and rate of $[Ca]_i$ transient decline accelerated until a new steady-state was reached. (B) Typical steady-state $[Ca]_i$ transients from an experiment where the pipette was loaded with 4 mM Ca. Steady-state $[Ca]_i$ at the indicated distances before high Ca addition are on the left. After Ca addition to the end of the cell (right), the peak steady-state $[Ca]_i$ increased most strongly underneath the pipette. The increase in peak $[Ca]_i$ along the scan line became progressively lower the farther upstream from the pipette that the measurement was taken.

with distance away from the pipette (Figure 3A and C).

Figure 3(A) illustrates the time course of Ca transient over 70 s (35 beats) postapplication of 4 mM Ca, which was very rapid at x = 0 and still quite rapid at x = 30 μm, quickly reaching steady-state. This is well-explained by immediate local increased influx via LTCC near the pipette, followed by adjustment of SR Ca loading over the next several beats.[28] Spatial spread of the response away from the pipette was indicated by the time required for the Ca transient amplitude to reach half of its steady state level (t_{50}; blue trace in Figure 3D left). On average, time required for half-maximal Ca transient increase was very rapid at x = 0 μm (2.1 ± 0.46 s) and still quite fast even 35 μm away (3.5 ± 1.2 s. at 35 μm away, *t*-test, $P < .05$). Although the increase in Ca transient amplitude fell substantially with distance (Figure 3C), the steady state spatial gradient of Ca transient amplitude was substantial between x = 0 and 30 μm. We attribute this to fast, but only partial, spatial redistribution of Ca within the SR,[29] such that SR Ca loading is elevated to some degree upstream from x = 0, where the local higher Ca current entry is unaltered, but a new steady state is rapidly achieved.

The half-time of twitch $[Ca]_i$ decline was not appreciably altered upon the high Ca switch and did not change as distance away from the pipette increased, indicating that the kinetics of Ca removal (mainly uptake of Ca into the SR but also efflux of Ca via Na/Ca exchange) was not different as a function of space (Figure 4B, left, blue trace; right, blue bars comparing x = 0 vs. 40 μm). The slightly faster Ca transient decay in high $[Ca]_o$ may be related to the faster time constant of $[Ca]_i$ decline intrinsic to larger Ca transients[30] and possible action potential duration changes.

Effects of Spatially Localized Increased ISO Upon the Cardiac Myocyte

Having tested the system by local $[Ca]_o$ increase, we used the same protocol with ISO in the pipette. Figure 2(A) shows the experimental arrangement and global $[Ca]_i$ recording. Figures 3(B) and 4(A) show the ISO-induced spatiotemporal increase Ca transient amplitude and acceleration of twitch $[Ca]_i$ decay over time post-ISO application.

As with high Ca exposure, ISO increased peak $[Ca]_i$ magnitude, as expected (Figure 3B). Steady-state peak $[Ca]_i$ under the pipette after ISO exposure increased by 88.5 ± 11.3% relative to pre-ISO levels at x = 0. The extent of Ca transient increase dissipated over distance away from the pipette, but the spatial extent of β-AR effect on Ca transient amplitude was greater than was the case with high $[Ca]_o$ (Figure 3C). That is, at x = 23 μm the Ca transient increase for ISO was still 70.4 ± 4.2% of the x = 0 level, whereas for 4 mM $[Ca]_o$ that increase was only 50.9 ± 6.4% of the x = 0 value (dashed lines in 3C; *t*-test, $P < .05$). Furthermore, in contrast to the case with high Ca-treatment, the half-times for myocytes to reach their maxima after ISO application were much slower, at x = 0 μm (15.7 ± 3.3 s) and significantly longer at x = 35 μm (26.5 ± 4.5 s; Figure 3B and D; *t*-test, $P < .05$). Notably, these values are roughly ten times longer than seen for the local 4 mM $[Ca]_o$ application.

Time to 50% Ca transient decline was also measured as a local readout of the rate of SR Ca uptake (Figure 4A).[31] Faster Ca transient decline due to PLN phosphorylation is a functional hallmark of β-AR dependent PKA activation—one that is robust and readily measurable. As with Ca transient amplitude

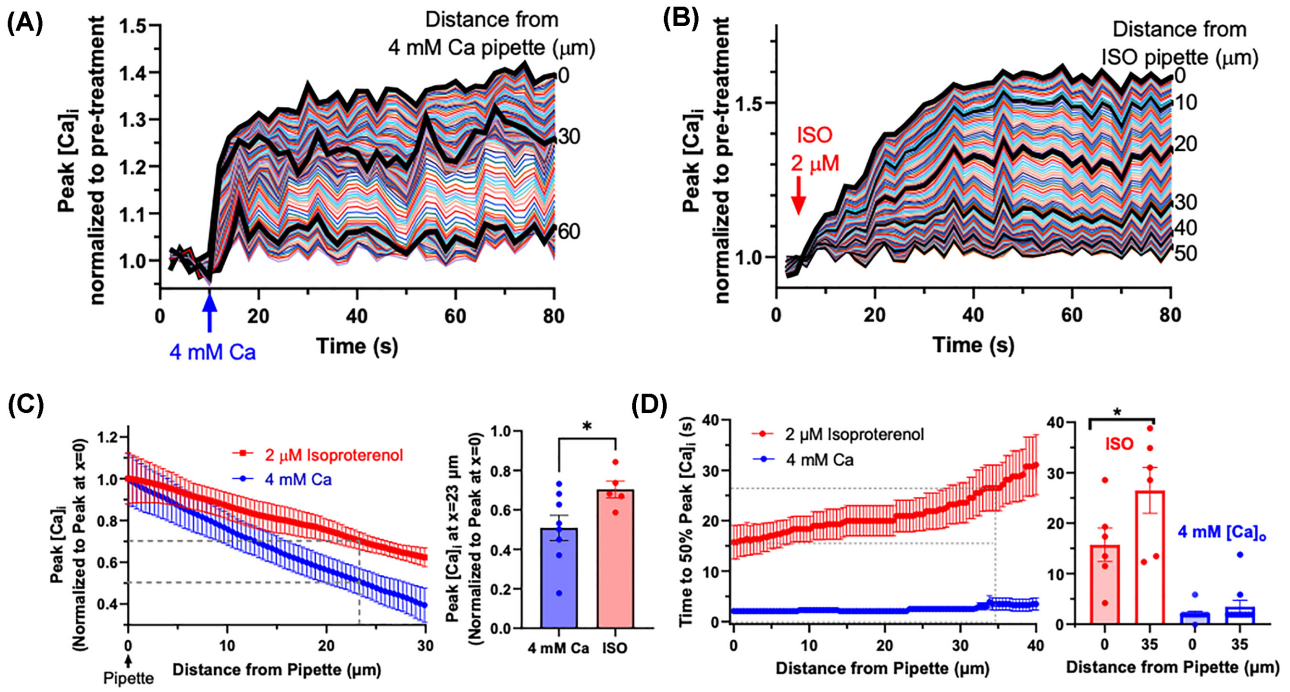

Figure 3. (A) The change in peak $[Ca]_i$ in response to local extracellular 4 mM Ca. High Ca was added locally at one end of the cell. Each line represents the change in Ca transients over space, from just underneath the pipette ("0 μm") with increasing distance upstream from that site. Upon high Ca addition, the peak $[Ca]_i$ underneath the pipette rose rapidly toward its new steady-state. As distance away from the pipette increased, the new steady-state peak $[Ca]_i$ became less. (B) Similar to (A), but with 2 μm ISO in the pipette rather than 4 mM Ca. ISO-induced increase in peak $[Ca]_i$ was far slower to reach steady state. (C) Peak $[Ca]_i$ as a function of distance upstream from the pipette (blue: 4 mM Ca; red: ISO). The ISO effect was more sustained over distance than the effect of high [Ca], with fractional increase in peak $[Ca]_i$ at 23 μm upstream marked by dotted lines and in bar graph, *t*-test, $P < .05$). (D) Converse plot of the time required for peak $[Ca]_i$ to reach 50% of its final, steady-state increase as a function of distance away from the pipette (left; blue: 4 mM Ca; red: ISO). The response to 4 mM Ca was very rapid (< 5 s) and minimally distance-dependent. In contrast, the ISO response developed much more slowly (15–30 s) and was significantly slower at longer distances from the pipette, with values at x = 0 and 35 μm shown by dotted lines and bar graph (*t*-test, $P < .05$).

increases, ISO-induced acceleration of twitch $[Ca]_i$ decline progressed, starting at x = 0 μm, to reach a steady-state spatial gradient within 60–80 s (Figure 4A).

At the pipette, ISO accelerated $[Ca]_i$ decline 2-fold (t_{50} decreased to 47 ± 5% of the pre-ISO value) and about half as much at x = 40 μm upstream (to 66 ± 5%; Figure 4B), measured at the time the curves in Figure 4(A) reached steady state. As with the rise in Ca transient amplitude, the kinetics of ISO-induced acceleration of twitch Ca transient decline in Figure 4(A) were also distance-dependent, averaging 24.0 ± 3.1 s at 0 μm vs. 36.4. ± 7.5 s at x = 40 μm). This can be contrasted with the time to 50% decline for the high Ca-treated cells, which was minimally hastened and did not change with distance away from the pipette.

Overall, ISO had the expected effects upon the myocyte, increasing peak $[Ca]_i$, and accelerating the rate of transient decline. The results are consistent with the involvement of the cAMP-PKA second messenger system, in that the ISO response developed more gradually within the myocyte than the 4 mM Ca response, and with a pronounced distance dependence with respect to the local application point. It was not surprising that the high-Ca effect propagated upstream from the pipette, because the higher Ca current entry at the pipette end could load Ca locally into the cell, which could mix and diffuse with other Ca in the cytosol and SR.[29,32] On the other hand, the strength of ISO responses was remarkably more maintained over distance, when compared to high Ca. These results suggest that the β-AR response involves active signaling that propagates up the cell away from the site of ISO exposure. While this could involve diffusion of cAMP[13] and/or PKA upstream in the myocyte, another possibility is the presence of intracellular β-AR that can be accessed by intracellular ISO that entered the myocyte at the downstream end.[21]

Signal Generation From Internalized β-receptors

Recent evidence has clearly shown the presence of intracellular myocyte β-ARs that can participate in accelerating SR Ca uptake due to local signal generation.[21] To test this hypothesis here, with a physiological agonist, we used 200 nM NE, which unlike ISO must be transported into myocytes, in the presence and absence of pretreatment by β-AR antagonists propranolol (1 μM), which is highly cell membrane permeant, and sotalol (25 μM), which is not membrane permeant.[21,33]

Very similar to ISO, local NE application alone caused the gradual evolution of a typical β-AR response. That is, rate of SR Ca uptake gradually accelerated (Figures 5A and 6B) to almost the same extent as seen with ISO in Figure 4, and the Ca transient peaks increased by 25.3 ± 6.2% (Figure 6A). Indeed, the half-time of Ca transient decline gradually decreased over 20 s during the application, falling to 34.7 ± 2.8% of the pre-NE value at x = 0 (Figures 5A, D, and 6B), with less effect further from the pipette (falling only to 68.7 ± 4.3% at x = 40 μm). The change in twitch $[Ca]_i$ decline also evolved more slowly over time with distance from the pipette to x = 40 μm (half-time of 22.0 ± 0.6 s and 30.3 ± 2.7 s, respectively—again similar to those seen with ISO in Figure 4).

When myocytes were pretreated with 1 μM propranolol and the protocol was repeated, the NE-dependent increases in Ca

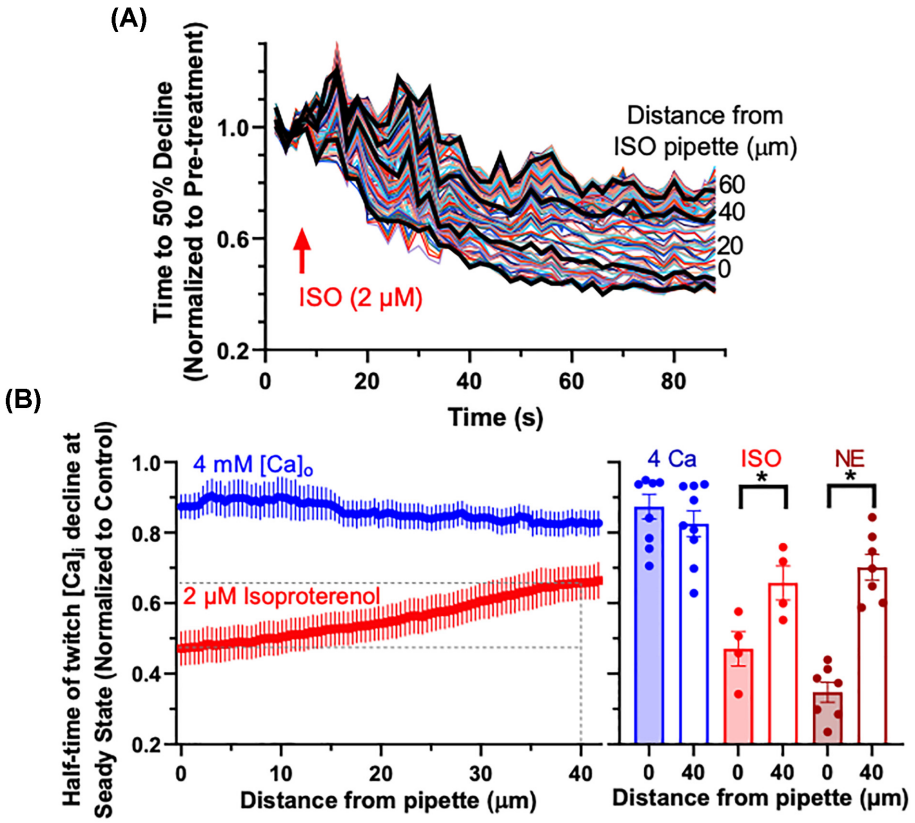

Figure 4. (A) Half-time of twitch $[Ca]_i$ decline as a function of time after ISO addition. Ca decline rate increased most strongly underneath the pipette (0 μm) where the increase was > 50% of preagonist control. The acceleration of Ca transient decline time became less as distance away from the pipette increased. (B) Distance-dependence of half-time of twitch $[Ca]_i$ decline at the steady state time point. For ISO, the steady-state rate of $[Ca]_i$ decline was fastest under the pipette (x = 0 μm), but the acceleration was weaker 40 μm upstream of ISO application, contrasting with the response to local 4 mM Ca, which was not distance-dependent. Steady state changes in Ca transient decline at x = 0 and 40 μm are shown as dashed lines for ISO at left, and as bars at right for 4 mM Ca, ISO, and NE (see also Figure 5A), Comparisons are by paired *t*-test (*P < .05).

transient amplitude and rate of decline were abolished (Figures 5B and 6A and B). This is consistent with complete β-AR blockade by the cell membrane permeant propranolol. In contrast with this response, when myocytes were pretreated with 25 μM sotalol to selectively block surface β-ARs, the NE response was only partially blocked (Figures 5C and D and 6A and B). Although to a much lesser extent compared to NE alone, NE with sotalol continued to accelerate Ca transient decline (at steady state to 74.7 ± 5.0% of pre-NE level, Figures 5C and 6B, *t*-test, $P < .05$). With sotalol, the ability of NE to shorten the Ca transient decline was weaker and occurred only gradually with increased distance from the pipette (Figure 5C and D). Sotalol, even at 25 μM, appeared to only partially block the NE-induced increase in Ca transient amplitude (only a 14.0 ± 1.5% increase from the pre-NE level, Figure 6(A), gray bar, *t*-test, $P = .13$). Although Ca transient decline was accelerated with NE ± sotalol, the evolution of this response in the presence of sotalol during an experiment, recorded at position 0 μm from the agonist pipette, was considerably slower than with NE alone (Figure 5D).

The data suggest that internalized β-AR may play a role in the evolution of the response to NE within cardiac myocytes. This response to internal β-ARs is smaller and slower to evolve. This is likely because activatable internal β-ARs represent only a fraction of total β-ARs, and because of time lags for NE transport into the myocyte and subsequent internal diffusion.

To test whether the partial acceleration of twitch $[Ca]_i$ decline in NE + sotalol required increased SR Ca uptake, we prevented SR Ca uptake by 25 min pretreatment with 5 μM thapsigargin. In rabbit ventricular myocytes, 5 μM thapsigargin abolishes SR Ca uptake within 2 min, but allows slower Ca transients that depend on Ca influx via Ca current (and Na/Ca exchange) and Ca efflux via Na/Ca exchange.[34] Consistent with the expected complete block of SR Ca uptake, the NE-induced acceleration of twitch $[Ca]_i$ decline was abolished with NE alone, and also with sotalol pretreatment. (Figure 6D). Despite prevention of SR Ca-uptake in thapsigargin, NE still induced a small increase in Ca transient amplitude (Figure 6C), but that is to be expected due to increased L-type Ca current, even without SR Ca uptake. Even sotalol-treated myocytes exhibited some NE-induced increase in Ca transients, but that may still reflect internal β-AR that can signal to Ca channels. Sotalol also inhibits a K^+ channel (I_{Kr}) that can prolong action potential duration and thus slows extrusion via Na/Ca exchange. We conclude that though the internalized β-AR can mediate an increase in SERCA2 activity (blocked by thapsigargin ± sotalol, Figure 6D, both bars), they may also generate intracellular second messengers which can alter the events at the plasma membrane.

AKAP7 May Also Contribute to Spatial Propagation of β-AR Signaling Along the SR

Most AKAPs are anchored at cellular sites in very close proximity to their targets.[7,8] However, AKAP7γ binds to the PKA target PLN, and the affinity of that interaction is reduced when PLN is

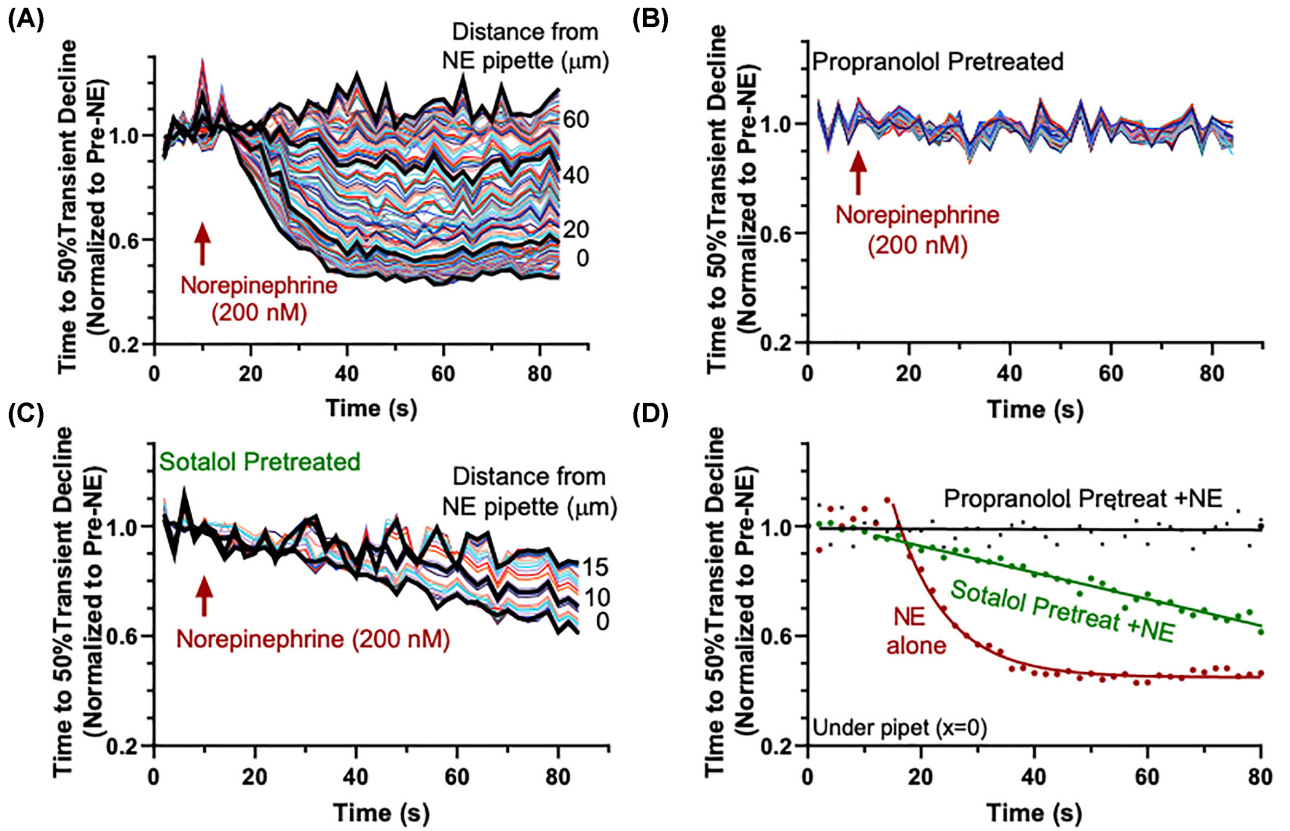

Figure 5. (A) The kinetics of $[Ca]_i$ decline as a function of time after 200 nM NE addition. As with ISO, the time to 50% decline decreased most strongly underneath the pipette and the effect lessened with distance away from it. (B) and (C) Half-time of $[Ca]_i$ decline as a function of time upon local NE application (200 nM) after pretreatment with 1 μM propranolol (B) or 25 μM sotalol (C). Sotalol, which blocks surface receptors only, reduced but did not eliminate the effect of the NE. (D) Comparison of twitch $[Ca]_i$ decline changes upon NE alone and with propranolol or sotalol pretreatment.

phosphorylated by PKA at Ser16.[15,16] That might allow AKAP7γ to function as a mobile AKAP that helps direct PKA to PLN along the SR surface.

To test AKAP7 mobility in adult rabbit ventricular myocytes we expressed GFP-tagged AKAP7γ via adenovirus and measured fluorescence recovery after photobleach (FRAP). Figure 7(A) shows that AKAP7γ-GFP expresses in a pattern much like PLN-YFP in the myocyte, consistent with AKAP7γ being especially concentrated at the SR. Regions of interest (ROIs) 10 μm in size were photobleached and FRAP for AKAP7γ-GFP was fairly rapid. By 65 s, the ROI structural organization was largely restored (exemplar in Figure 7B, left). However, FRAP was only ~85% complete, indicative of some relatively immobile AKAP7γ as well (Figure 7B). In comparison, FRAP of YFP-PLN is slower and exhibits a higher immobile fraction. While PLN is less mobile than AKAP7γ, it is notable that this small membrane protein is able to translocate within the confines of the SR network. The fast tau of AKAP7γ-GFP recovery was ~10 s, compared to 4.6 ± 1.0 for GFP alone (which is roughly half the size) measured in parallel experiments (not shown). This fast tau may reflect an AKAP7γ fraction that is freely mobile or binds with modest affinity to targets. The longer tau (100 s) might reflect both slower off-rates from AKAP7γ binding partners, but also diffusion from longer distances away.

Initial FRAP studies of AKAP7γ-GFP upon ISO exposure, failed to discern consistent changes in FRAP kinetics. As an alternative, we instead directly measure AKAP7γ-GFP washout upon plasma membrane saponin-permeabilization. Figure 8(A) shows that GFP washes out much faster than AKAP7γ-GFP (tau of ~50 and 350 s, respectively). Part of that difference may be attributable to the 2-fold difference in molecular size, but when forskolin was added to AKAP7γ-GFP expressing myocytes, the washout was much faster (tau = 193 s; Figure 8B). In addition, the mean residual AKAP7γ-GFP fluorescence (asymptotic plateau of exponential fits) was also greatly reduced after forskolin treatment. Taken together, these data would be consistent with a PKA-dependent enhancement of AKAP7γ mobility that might be expected by the reduced affinity of AKAP7γ to PLN when PLN is phosphorylated.

Discussion

The β-AR system is a central mechanism in regulating cardiac function by a richly orchestrated cascade of PKA-dependent phosphorylation myocyte protein targets that cause increased heart rate (chronotropy), contractile strength (inotropy), relaxation rate (lusitropy), and conduction velocity (dromotropy) that are major players in the rapid sympathetic fight-or-flight response.[2] Cardiac β-AR responsiveness is also blunted in cardiac disease states including most forms of HF,[4] where β-AR antagonists are a standard treatment and can partially restore sympathetic responsiveness and improve survival.[5,35] Notably, adrenergic signaling in the heart occurs at local sites of NE release (or varicosities) along myocytes, rather than the global bath or perfusate exposure that is often used experimentally.[25]

Our novel methods and data demonstrate how the locally initiated β-AR activation response (via ISO and NE) propagates over

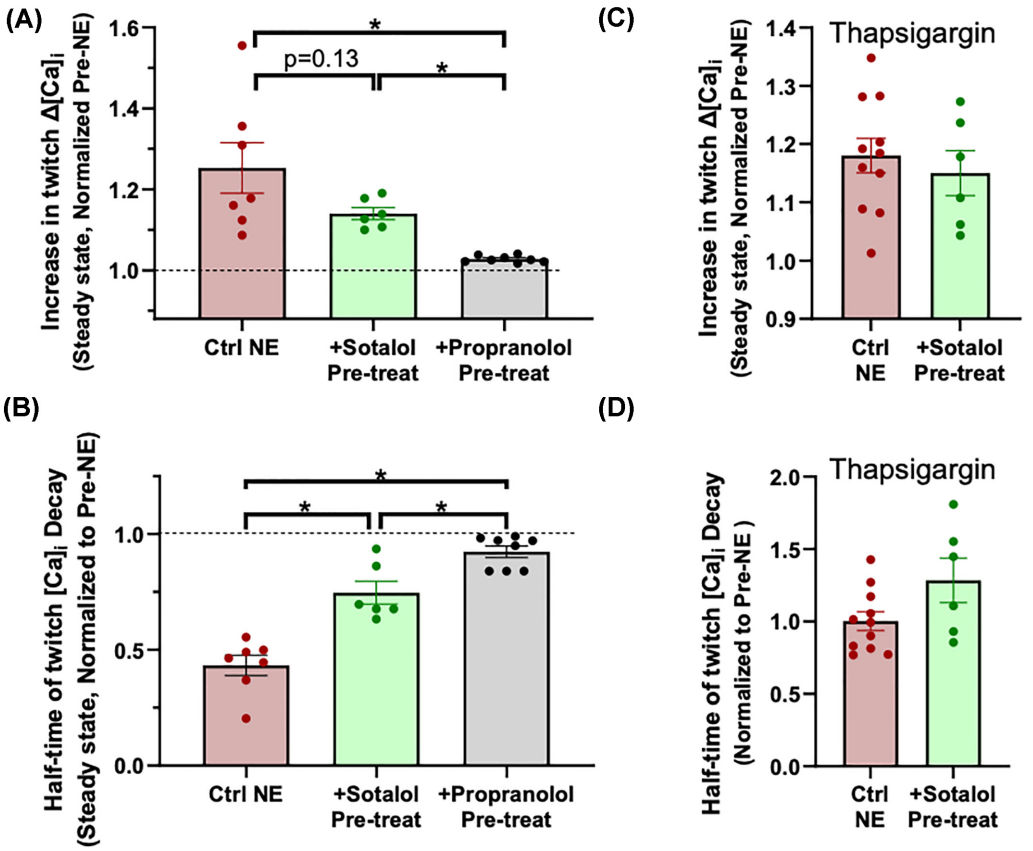

Figure 6. (A) and (B) Steady-state peak $[Ca]_i$ (A) and time to 50% decline (B) in response to 200 nM local NE with and without 25 μM sotalol or 1 μM propranolol. Propranolol, which is membrane permeant, completely blocked NE effects. Sotalol, which blocks only the surface receptors, only partially blocks the time to 50% decline. The residual NE effect is consistent with the hypothesis that internal receptors are still available to bind NE in the presence of excess sotalol. (C) and (D) The same experiment after pretreatment with thapsigargin. Thapsigargin completely inhibited the decrease in the time to 50% decline, indicating that SR Ca uptake was eliminated regardless. Nevertheless, treatment with sotalol did not completely block the increase in the $[Ca]_i$ transient, which could be due to increased I_{Ca}. The data suggest that NE binding to internal receptors still generates second messengers, which may diffuse back to cause effects at the plasma membrane.

both time and space longitudinally in the adult myocyte. Compared to a local increase in $[Ca]_o$, the β-AR response is more gradual to develop, but spreads throughout the myocyte more extensively. The local NE effect was abolished by the membrane permeant β-AR antagonist propranolol, but not by sotalol (which is expected to selectively block surface β-ARs).[21] We conclude that β-AR signal propagation in myocytes is facilitated by activation of intracellular β-AR that accelerate SR Ca uptake (Figure 9A). Our data also suggest the involvement of internal β-AR receptors in the response, which are associated with both increased SR Ca uptake and increased L-type Ca current in the case where SR Ca uptake was blocked.[21]

AKAP7γ (or -δ) interacts with PLN and facilitates PKA-dependent phosphorylation of PLN and the consequent enhanced SR Ca uptake in heart.[7,15–17] Here, we showed that AKAP7γ has high mobility in cardiac myocytes, unlike most AKAPs, which as their name implies, tend to anchor PKA with functional partners at specific myocyte locations. This raises a novel working hypothesis that AKAP7γ may exert its function on SR Ca uptake in part because of this mobility (Figure 9). Moreover, AKAP7γ mobility and intracellular β-ARs may both contribute locally to the rapid intracellular spread of SR Ca uptake enhancement that critically mediates the cardiac fight-or-flight response.

Local $[Ca]_o$ Elevation Creates a Standing Gradient of Ca Transients in Myocytes

The rapid response to local 4 mM $[Ca]_o$ also spreads very quickly throughout the cell despite the restriction of increased L-type Ca current to the area underneath the pipette. It did surprise us that this rapidly established a standing gradient of Ca transient amplitudes along the myocyte (Figure 3A and C). We expect this high $[Ca]_o$ to load the myocyte and SR locally where $I_{Ca,L}$ is increased. But there is also greater Ca transients amplitude, which over just a few beats drives a new steady-state, where Ca extrusion per beat exactly balances Ca influx.[37] Thus, the time-averaged cytosolic and SR [Ca] may be less changed than one might intuit. In addition, Ca diffusion is rapid within the SR network[36] partly because of the high intra-SR [Ca] ($[Ca]_{SR}$; > 5000 times that of $[Ca]_i$) that drives greater flux, proportional to ($[Ca]_{high}$—$[Ca]_{low}$). Thus, a tendency for Ca to diffuse from a slightly higher diastolic $[Ca]_{SR}$ in the high $[Ca]_o$ end, would reverse during SR Ca release and deeper $[Ca]_{SR}$ depletion (and reciprocally in the cytosol). Finally, there may be relatively small changes in SR Ca content, because net cellular Ca gain is restricted to the first few beats, such that local Ca transients (or fractional release) are regulated mainly by the amplitude of the local $I_{Ca,L}$ trigger. That may allow very different amplitude local

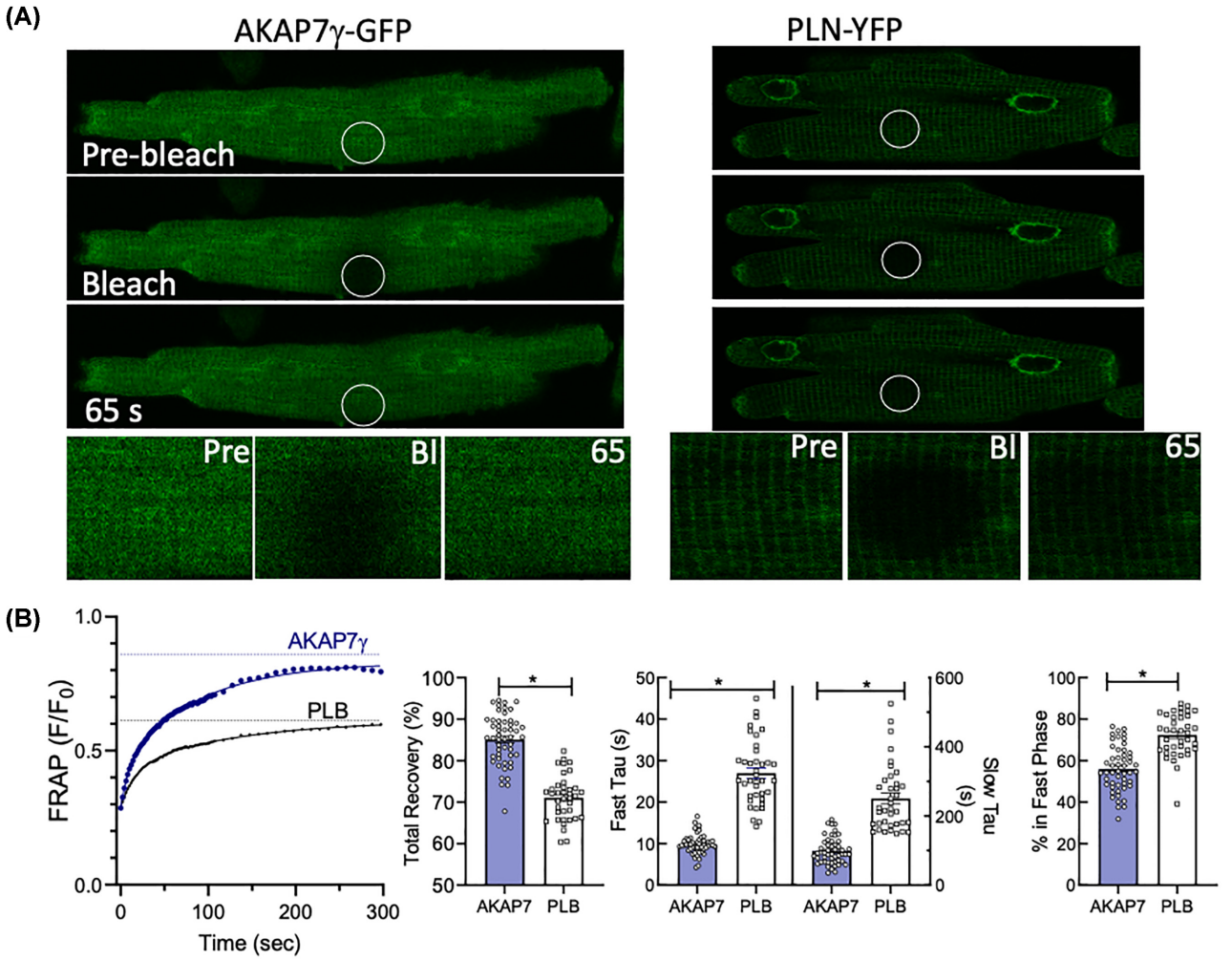

Figure 7. (A) Examples images of FRAP experiment showing AKAP7γ-GFP (left) and a YFP-PLN transfected cell (right) before bleaching, immediately after bleaching and after 65 s of recovery. The bleach area is indicated with a white circle and is enlarged in the lower images. (B) Representative traces of FRAP resulting from analyzing such images for AKAP7-GFP and PLN-YFP (dashed lines show mean total recovery % from next panel). Traces were fit by two-phase association fit. Summary data showing the % total recovery, the fast and slow time constants (tau) of recovery, and the % recovery of the fast phase only are shown to the right. Analysis from $n = 51$ cells from $N = 5$ hearts (AKAP7-GFP) and $n = 38$ from $N = 6$ (PLN-YFP) $^*P < .05$.

Ca transients (and amounts of Ca influx that matches efflux) to coexist in this steady state.

Time-Dependent Propagation of β-AR Response in Myocytes

The response to ISO in our experiments was slow by comparison to high $[Ca]_o$, half-maximal in ~15 s (vs. 3 s), even under the pipette (Figures 3 and 4). Time-dependence of agonist binding to surface β-AR receptors underneath the pipette could contribute, but the high ISO and NE concentrations we used should minimize this. So, most of this local delay is likely due to the many biochemical steps between β-AR binding and our effector readouts of Ca transient amplitude and decay (26.5 and 24 s half-times, respectively). Those steps include G-protein activation, consequent adenylyl cyclase activation, cAMP production, binding to PKA regulatory subunit, and PKA-dependent phosphorylation of targets (eg, L-type Ca channel and PLN). These activating effects are also limited by phosphodiesterases that break down cAMP and phosphatase that dephosphorylate targets. Based on the short lag for abrupt increase in $[Ca]_o$ (~2 s), most of this β-AR signaling lag may precede the actual Ca-flux changes. Having said that, in rabbit ventricular myocytes ISO increases Ca current ($I_{Ca,\,L}$) with a halftime of ~7 s, whereas the delayed K^+ current (I_{Ks}) increases with a half-time of ~30 s (both of which are facilitated by AKAPs), and that kinetic delay between $I_{Ca,\,L}$ and I_{Ks} activation can cause a vulnerable time window with respect to arrhythmogenesis.[38,39] The rate of SR Ca uptake, which we infer from the half-time for tau of $[Ca]_i$ decline (24 s) is more in-line with that for I_{Ks}, and signaling to the myofilaments PKA targets may be even slower.[11] This emphasizes that $I_{Ca,\,L}$ has the shortest lag for β-AR modulation, indicative of most efficient coupling from β-AR to function. But not all sarcolemmal targets are that fast (eg, I_{Ks}), which is consistent with the concept of highly localized nanodomains in which complex cAMP and PKA regulation occurs.[11,40]

The longitudinal propagation rate of SR Ca-ATPase β-AR effects that we observed was approximately 3.2 μm/s (Figure 3D), and this should be mediated by events inside the myocyte, since that part of the cell is not exposed to β-AR agonist because of the overwhelming bulk fluid flow. Propagation of myocyte cAMP

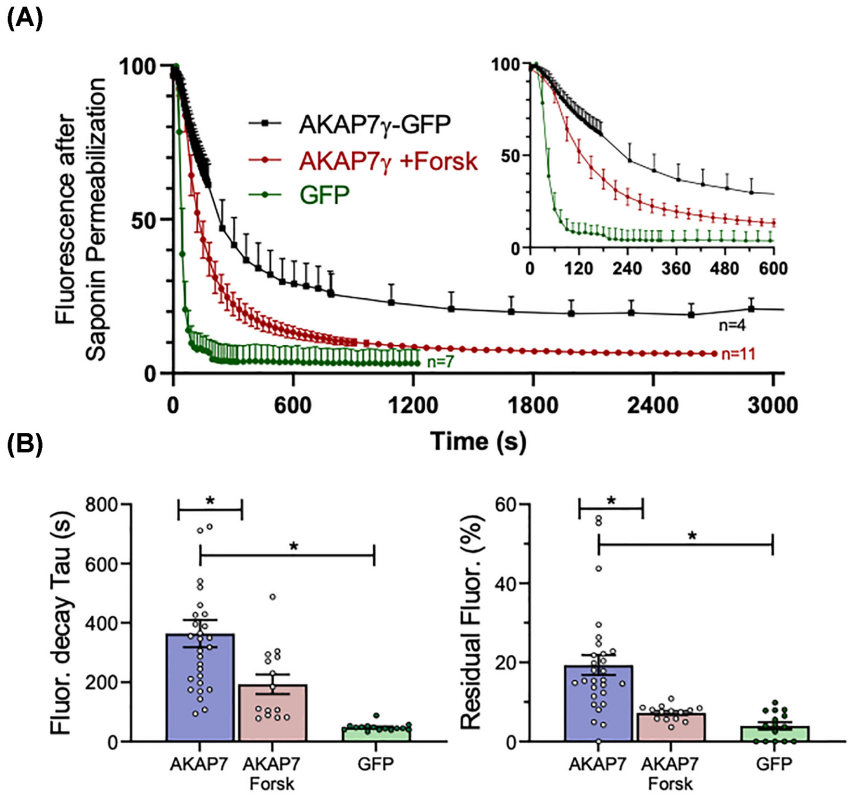

Figure 8. Washout of AKAP7-GFP upon saponin-permeabilization of adult rabbit ventricular myocytes. (A) Fluorescence decay in three exemplar subsets of myocytes (AKAP7γ-GFP, AKAP7γ-GFP + Forskolin, and GFP) where fluorescence measurements had been taken at identical time points (*n* values indicated). Inset shows expanded first 10 min. (B) Time constants of fluorescence decay upon saponin permeabilization (left) and residual fluorescence plateau (right) from monoexponential curve fits of data like that in panel (A). Analysis was from *n* cells/*N* animals: 28/5 for AKAP7-GFP, 15/3 for AKAP7γ+Forskolin, and 15/3 for GFP $^*P < .05$.

levels have been reported to be as fast as 15 μm/s upon β_1-AR activation,[13] which is faster than the propagation of β-AR to our measured SR Ca-uptake. However, the ability of PDE inhibitors to enhance the physical spread of cAMP signal target effects might mean that the cAMP sensors themselves can diffuse and protect cAMP from PDEs.[2] In addition, some component of this longitudinal signal propagation could be mediated by slower activation of intracellular β-ARs,[19–23] or the movement of active PKA on AKAP7γ to phosphorylate targets like PLN,[7,15–17] or both.

Intracellular β Receptors Can Mediate the Adrenergic Response

Wang et al. recently showed that some myocyte β-AR receptors are localized inside the myocyte at the SR with SERCA2 in mouse cardiomyocytes.[21] They suggested that these intracellular β-ARs had preferential effects on upon SR Ca uptake (Figure 9). Both PLN phosphorylation and SR-associated PKA activity were attenuated when NE transport into the cell was eliminated in OCT3 KO mice. They also found that SR-associated PKA activity was preserved in control hearts when only surface β-AR receptors were blocked with sotalol, but all β-AR effects were blocked when the membrane-permeant blocker propranolol was used. Our data support and extend these results. Indeed, while propranolol abolished the NE response completely, when intracellular β-ARs were selectively activated (NE + sotalol) the spatiotemporal acceleration of SERCA2 function, though less robust, was still readily apparent. Recent studies have also suggested that activation of intracellular β-AR generates effects which depend upon the localization of the receptors.[19–21] In addition, β-AR activation-induced PKA activity in HF is inhibited at the SR and myofilaments, but not at the plasma membrane.[11,12]

To test that the internal β-AR response required SERCA2 function, we used thapsigargin to completely prevent SR Ca uptake. With or without sotalol, NE could not hasten Ca transient decline (Figure 6D), but we did see a small NE-dependent increase in peak $[Ca]_i$, even with 25 μM sotalol. This indicates that at least some residual effect of NE on $I_{Ca,L}$ remained, which is likely to have been mediated by intracellular β-ARs (consistent with its slow emergence vs. rapid β-AR-induced Ca current activation[38]). We cannot say how efficient the full signal transduction cascade is from intracellular β-AR via G_α-AC-cAMP-PKA and AKAP to the Ca channel or SERCA (compared to that via surface β-ARs) or how much local PDE and phosphatases may limit target phosphorylation. What we can say is that despite the intrinsic complexity, we can directly observe spatiotemporal functional effects via intracellular β-AR on SR Ca uptake. Thus, while our data are consistent with a preferential effect of internal β-AR on the SR, this preference is not absolute.

The potential implications of a sustained spatial gradient of response away from a local site of activation are useful to consider. In vivo, sympathetic activation of in cardiac myocytes is caused mainly by NE released from autonomic nerve endings called varicosities. These endings impinge on distinct local areas of the cardiac myocyte (unlike global bath application or bolus infusion of β-AR agonists used experimentally). The current data suggest that there can be inhomogeneities caused by local activation of the myocyte. Thus, multiple mechanisms

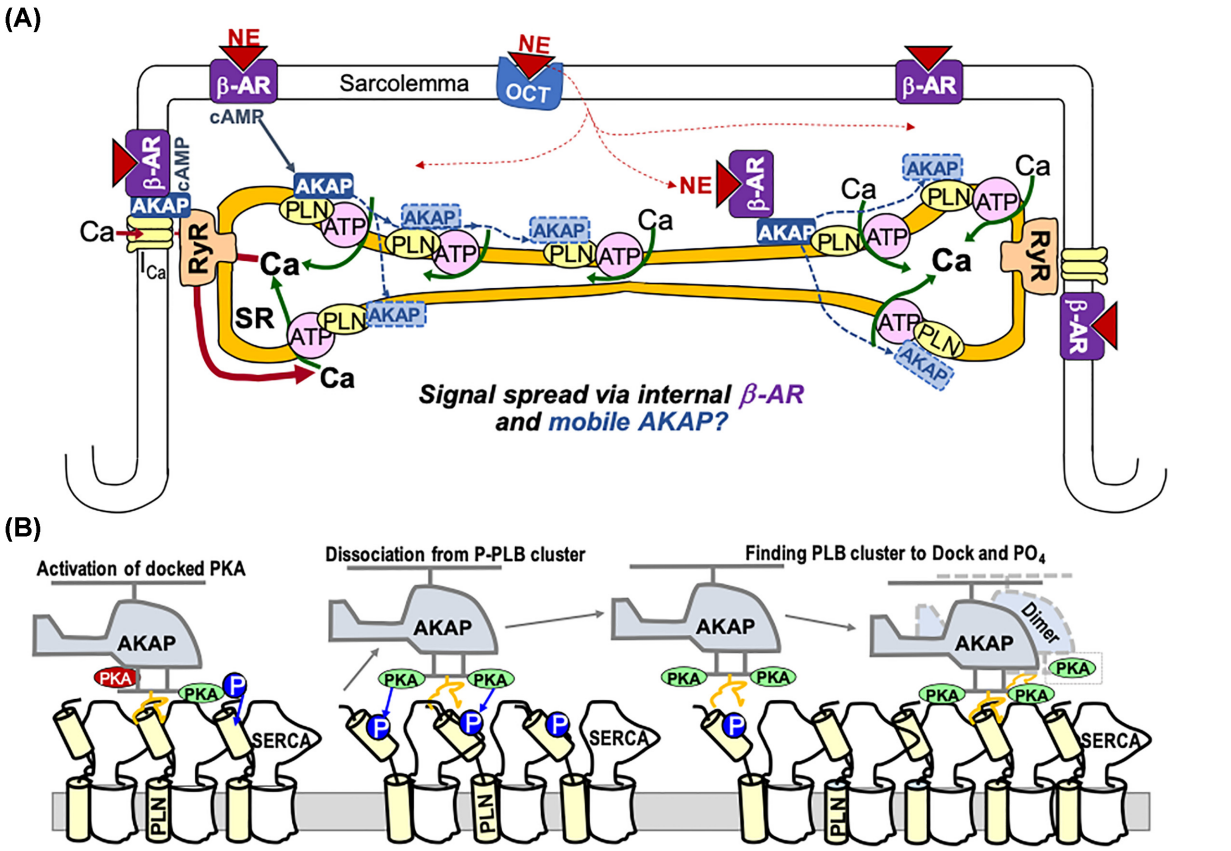

Figure 9. Working hypothesis for β-AR signal spread in myocytes. (A) Norepinephrine activates β-AR, which raises cAMP and activates myocyte PKA. Norepinephrine can enter via OCT, diffuse and activate intracellular β-ARs, contributing to PLN phosphorylation and acceleration of SR Ca uptake. AKAP7γ may shuttle active PKA along the surface of the SR membrane. Together these two mechanisms may facilitate rapid spatial β-AR signaling to SR Ca uptake. (B) AKAP7γ binds to PLN near its PKA phosphorylation site (Left). When inactive PKA (red) binds cAMP and becomes activated (green), it can phosphorylate nearby PLN (left to center). When all local PLN is phosphorylated (center), it reduces PLN-AKAP7γ affinity, facilitating dissociation. Active PKA-AKAP7γ can diffuse (hover) along the SR surface and quickly finds other clusters of unphosphorylated PLN to bind to and phosphorylate. AKAP7γ dimerization may help restrict this diffusion to the SR surface if only one monomer is released from the PLN at a time (hand-over-hand). Thus, AKAP7γ moves along the SR surface, rapidly phosphorylating PLN.

may help to spread β-AR signal uniformly within the myocyte and be beneficial in optimizing spatial synchrony of contraction with myocytes and the heart. Indeed, NE extracellular diffusion, transport into the myocyte and intracellular diffusion of NE, cAMP, and even AKAP7γ may contribute to the spreading of β-AR signal from nerve ending loci.

β-AR Phosphorylation Target PLN is Mobile, But AKAP7γ is More Mobile

PLN is a resident transmembrane SR protein, but it exhibits substantial mobility in the myocyte, as measured by FRAP (Figure 7). This reminds us that even proteins that we think of as constrained (in the SR) can move dynamically within the SR membrane. AKAP7γ exhibits higher mobility than PLN, and a exhibits a smaller apparently immobile fraction.

AKAP7 is synonymous with AKAP18 as products of the *Akap7* gene. This gene produces four splice variants (α, β, γ, and δ). AKAP7γ and δ are the two longer splice variants which function similarly. AKAP7γ is ancestral and the dominant splice variant in mouse and human heart (but is replaced by AKAP7δ in rat).[16,41] Lygren et al.[15] first showed that AKAP18δ interacts with PLN and facilitates PKA-dependent PLN phosphorylation and SR Ca uptake. More recent work indicates that PLN phosphorylation decreases the PLN affinity of AKAP7γ and that AKAP7γ also functions as a dimer.[15–17] Our data here are consistent with this, showing that AKAP7γ has similar cellular localization as PLN and is highly mobile in adult rabbit myocytes (Figure 7), and that PKA activation (to phosphorylate PLN) accelerates AKAP7γ mobility as evidenced by faster diffusion from and reduced residual concentration in saponin-permeabilized myocytes (Figures 7 and 8).

Working Hypothesis for Intracellular β-AR and AKAP7γ Roles in SERCA2 Regulation

Together, our data and that of others lead us to a working hypothesis schematized in Figure 9. β-AR activation promotes cAMP and PKA activation in the myocyte, and this is critical for the enhanced $I_{Ca,L}$ via a canonical AKAP pathway. While rapid cAMP diffusion that is PDE-sensitive may help spread globally, local fixed AKAP signaling seems inadequate to explain rapid stoichiometric PLN phosphorylation and the rapid stimulation of SR Ca uptake. We hypothesize two additional mechanisms add to this (Figure 9A). First, intracellular β-ARs that further promote PKA activation at the network SR (and possibly the myofilaments). Second, mobile AKAP7γ that may shuttle active PKA along the surface of the SR membrane, mediating PLN phosphorylation and acceleration of SR Ca uptake locally. Figure 9B clarifies the latter hypothesis in that at rest some AKAP7γ sits

bound to PLN. Then upon cAMP-dependent activation of PKA (green vs. red; left) with PKA catalytic subunit loosely bound to the regulatory AKAP complex,[14,42–44] PKA can phosphorylate all nearby PLN, which reduces PLN-AKAP7γ affinity.[16] The more favored dissociation (center) then allows AKAP7γ-PKA to hover along the SR quickly finding clusters of unphosphorylated PLN to bind to and phosphorylate (right). This model would allow AKAP7γ to move along the SR surface, rapidly phosphorylating PLN as it goes. Importantly, AKAP7γ dimerization[17] might constrain AKAP7γ to move along the SR surface rather than diffuse randomly in the cytosol once released (ie, 2D surface vs. 3D diffusion). While speculative, this model may help focus further studies.

In summary, this study elucidates a novel signaling paradigm in which intracellular β-ARs and possibly AKAP7γ participate in β-AR stimulation of cardiac myocytes. Local stimulation of both surface and intracellular receptors may limit physiologically the spatial gradients that we have revealed in the myocyte by focal activation of β-AR. This signaling ensemble may become dysregulated in pathophysiological situations, undermining physiological synchronizing effects in β-AR signaling.

Acknowledgments

We thank Sonya Baidar for preparation of adenoviruses used to express AKAP7γ and PLN fusion in adult cardiac myocytes and Logan R. Bailey and Johanna Borst for isolation of myocytes and general laboratory support.

Funding

This work was supported by the NIH grants R01HL133832, P01-HL141084 (DMB), R01-HL126825, and R01-HL153835 (K.D.K.), the NIH HL147263 and VA Merit grant 01BX005100 (Y.K.X.).

References

1. Lymperopoulos A, Rengo G, Koch WJ. Adrenergic nervous system in heart failure: pathophysiology and therapy. *Circ Res*. 2013;**113**(6):739–753.
2. Bers DM, Xiang YK, Zaccolo M. Whole-cell cAMP and PKA activity are epiphenomena, nanodomain signaling matters. *Physiology*. 2019;**34**(4):240–249.
3. Bristow MR, Ginsburg R, Minobe W, et al. Decreased catecholamine sensitivity and beta-adrenergic-receptor density in failing human hearts. *N Engl J Med*. 1982;**307**(4):205–211.
4. Lohse MJ, Engelhardt S, Eschenhagen T. What is the role of beta-adrenergic signaling in heart failure?. *Circ Res*. 2003;**93**(10):896–906.
5. Bristow MR. Beta-adrenergic receptor blockade in chronic heart failure. *Circulation*. 2000;**101**(5):558–569.
6. Baldwin TA, Dessauer CW. Function of adenylyl cyclase in heart: the AKAP connection. *J Cardiovasc Dev Dis*. 2018;**5**(1):2. DOI: 10.3390/jcdd5010002.
7. Diviani D, Dodge-Kafka KL, Li J, Kapiloff MS. A-kinase anchoring proteins: scaffolding proteins in the heart. *Am J Physiol Heart Circ Physiol*. 2011;**301**(5):H1742–1753.
8. Dodge-Kafka KL, Langeberg L, Scott JD. Compartmentation of cyclic nucleotide signaling in the heart: the role of A-kinase anchoring proteins. *Circ Res*. 2006;**98**(8):993–1001.
9. Xiang YK. Compartmentalization of beta-adrenergic signals in cardiomyocytes. *Circ Res*. 2011;**109**(2):231–244.
10. Nikolaev VO, Moshkov A, Lyon AR, et al. Beta2-adrenergic receptor redistribution in heart failure changes cAMP compartmentation. *Science*. 2010;**327**(5973):1653–1657.
11. Surdo NC, Berrera M, Koschinski A, et al. FRET biosensor uncovers cAMP nano-domains at beta-adrenergic targets that dictate precise tuning of cardiac contractility. *Nat Commun*. 2017;**8**(1):15031.
12. Barbagallo F, Xu B, Reddy GR, et al. Genetically encoded biosensors reveal PKA hyperphosphorylation on the myofilaments in rabbit heart failure. *Circ Res*. 2016;**119**(8):931–943.
13. Nikolaev VO, Bunemann M, Schmitteckert E, Lohse MJ, Engelhardt S. Cyclic AMP imaging in adult cardiac myocytes reveals far-reaching beta1-adrenergic but locally confined beta2-adrenergic receptor-mediated signaling. *Circ Res*. 2006;**99**(10):1084–1091.
14. Omar MH, Scott JD. AKAP signaling islands: venues for precision pharmacology. *Trends Pharmacol Sci*. 2020;**41**(12):933–946.
15. Lygren B, Carlson CR, Santamaria K, et al. AKAP complex regulates Ca2+ re-uptake into heart sarcoplasmic reticulum. *EMBO Rep*. 2007;**8**(11):1061–1067.
16. Rigatti M, Le AV, Gerber C, Moraru II, Dodge-Kafka KL. Phosphorylation state-dependent interaction between AKAP7delta/gamma and phospholamban increases phospholamban phosphorylation. *Cell Signalling*. 2015;**27**(9):1807–1815.
17. Singh A, Rigatti M, Le AV, Carlson CR, Moraru II, Dodge-Kafka KL. Analysis of AKAP7gamma dimerization. *J Signal Transduct*. 2015;**2015**(24):371626. DOI: 10.1155/2015/371626.
18. Saucerman JJ, Brunton LL, Michailova AP, McCulloch AD. Modeling beta-adrenergic control of cardiac myocyte contractility in silico. *J Biol Chem*. 2003;**278**(48):47997–48003.
19. Irannejad R, Pessino V, Mika D, et al. Functional selectivity of GPCR-directed drug action through location bias. *Nat Chem Biol*. 2017;**13**(7):799–806.
20. Nash CA, Wei W, Irannejad R, Smrcka AV. Golgi localized beta1-adrenergic receptors stimulate Golgi PI4P hydrolysis by PLCepsilon to regulate cardiac hypertrophy. *Elife*. 2019;**8**:e48167. DOI: 10.7554/eLife.48167.
21. Wang Y, Shi Q, Li M, et al. Intracellular beta1-adrenergic receptors and organic cation transporter 3 mediate phospholamban phosphorylation to enhance cardiac contractility. *Circ Res*. 2021;**128**(2):246–261.
22. Wright CD, Chen Q, Baye NL, et al. Nuclear alpha1-adrenergic receptors signal activated ERK localization to caveolae in adult cardiac myocytes. *Circ Res*. 2008;**103**(9):992–1000.
23. Vaniotis G, Glazkova I, Merlen C, et al. Regulation of cardiac nitric oxide signaling by nuclear β-adrenergic and endothelin receptors. *J Mol Cell Cardiol*. 2013;**62**:58–68.
24. Rose CP, Burgess JH, Cousineau D. Tracer norepinephrine kinetics in coronary circulation of patients with heart failure secondary to chronic pressure and volume overload. *J Clin Invest*. 1985;**76**(5):1740–1747.
25. Prando V, Da Broi F, Franzoso M, et al. Dynamics of neuroeffector coupling at cardiac sympathetic synapses. *J Physiol*. 2018;**596**(11):2055–2075.
26. Pogwizd SM, Schlotthauer K, Li L, Yuan W, Bers DM. Arrhythmogenesis and contractile dysfunction in heart failure: roles of sodium-calcium exchange, inward rectifier potassium current, and residual beta-adrenergic responsiveness. *Circ Res*. 2001;**88**(11):1159–1167.

27. Bidwell P, Blackwell DJ, Hou Z, Zima AV, Robia SL. Phospholamban binds with differential affinity to calcium pump conformers. *J Biol Chem*. 2011;**286**(40):35044–35050.
28. Diaz ME, Graham HK, O'Neill S C, Trafford AW, Eisner DA. The control of sarcoplasmic reticulum Ca content in cardiac muscle. *Cell Calcium*. 2005;**38**(3-4):391–396.
29. Picht E, Zima AV, Shannon TR, Duncan AM, Blatter LA, Bers DM. Dynamic calcium movement inside cardiac sarcoplasmic reticulum during release. *Circ Res*. 2011;**108**(7): 847–856.
30. Bers DM, Berlin JR. Kinetics of [Ca]i decline in cardiac myocytes depend on peak [Ca]i. *Am J Physiol*. 1995;**268**(1 Pt 1):C271–277.
31. Li L, Desantiago J, Chu G, Kranias EG, Bers DM. Phosphorylation of phospholamban and troponin I in beta-adrenergic-induced acceleration of cardiac relaxation. *Am J Physiol Heart Circ Physiol*. 2000;**278**(3):H769–779. http://www.ncbi.nlm.nih.gov/pubmed/10710345.
32. Wu X, Bers DM. Sarcoplasmic reticulum and nuclear envelope are one highly interconnected Ca2+ store throughout cardiac myocyte. *Circ Res*. 2006;**99**(3):283–291.
33. Detroyer A, Vander Heyden Y, Carda-Broch S, Garcia-Alvarez-Coque MC, Massart DL. Quantitative structure-retention and retention-activity relationships of beta-blocking agents by micellar liquid chromatography. *J Chromatogr A*. 2001;**912**(2):211–221.
34. Bassani JW, Bassani RA, Bers DM. Twitch-dependent SR Ca accumulation and release in rabbit ventricular myocytes. *Am J Physiol*. 1993;**265**(2 Pt 1):C533–540.
35. Ping P, Anzai T, Gao M, Hammond HK. Adenylyl cyclase and G protein receptor kinase expression during development of heart failure. *Am J Physiol*. 1997;**273**(2 Pt 2):H707–717.
36. Bers DM, Shannon TR. Calcium movements inside the sarcoplasmic reticulum of cardiac myocytes. *J Mol Cell Cardiol*. 2013;**58**:59–66.
37. Eisner DA, Choi HS, Diaz ME, O'Neill SC, Trafford AW. Integrative analysis of calcium cycling in cardiac muscle. *Circ Res*. 2000;**87**(12):1087–1094.
38. Liu GX, Choi BR, Ziv O, et al. Differential conditions for early after-depolarizations and triggered activity in cardiomyocytes derived from transgenic LQT1 and LQT2 rabbits. *J Physiol*. 2012;**590**(5):1171–1180.
39. Xie Y, Grandi E, Puglisi JL, Sato D, Bers DM. Beta-adrenergic stimulation activates early afterdepolarizations transiently via kinetic mismatch of PKA targets. *J Mol Cell Cardiol*. 2013;**58**:153–161.
40. Zhang JZ, Lu TW, Stolerman LM, et al. Phase separation of a PKA regulatory subunit controls cAMP compartmentation and oncogenic signaling. *Cell*. 2020;**182**(6):1531–1544.e1515.
41. Johnson KR, Nicodemus-Johnson J, Carnegie GK, Danziger RS. Molecular evolution of A-kinase anchoring protein (AKAP)-7: implications in comparative PKA compartmentalization. *BMC Evol Biol*. 2012;**12**(1):125.
42. Martin BR, Deerinck TJ, Ellisman MH, Taylor SS, Tsien RY. Isoform-specific PKA dynamics revealed by dye-triggered aggregation and DAKAP1alpha-mediated localization in living cells. *Chem Biol*. 2007;**14**(9):1031–1042.
43. Taylor SS, Ilouz R, Zhang P, Kornev AP. Assembly of allosteric macromolecular switches: lessons from PKA. *Nat Rev Mol Cell Biol*. 2012;**13**(10):646–658.
44. Smith FD, Reichow SL, Esseltine JL, et al. Intrinsic disorder within an AKAP-protein kinase A complex guides local substrate phosphorylation. *Elife*. 2013;**2**:e01319. DOI: 10.7554/eLife.01319.